Comparison Study of Singly-Fed Electric Machine with Doubly-Fed Machine for EV/HEV Applications

Longya Xu* Yu Liu* and Xuhui Wen**
*The Ohio State University, USA
**Inst. of Electrical Engineering, Chinese Academy of Sceinces, China
wxh@mail.iee.ac.cn

Abstract — A doubly fed motor performance is analyzed and experimentally tested. The performance of the doubly fed machine is compared for various operational conditions for variable speed applications. In particular, the possibility of eliminating brushes and slip rings for the doubly fed motor is also discussed and solution presented to highlight the bright future of the brushless doubly fed motor in EV/EHV applications.

I. INTRODUCTION

Technology development for HEV/EV motors has gone a long way and progressed tremendously for the last two decades. The key issues for a typical HEV/EV motor are a) torque density in terms of weight and volume; b) torque-speed capability; c) energy efficiency; d) reliability; and e) costs in manufacturing and maintenance. Currently, two types of electric motors are most popular: Interior Permanent Magnet (IPM) motor and cage induction motor (IM) with their drive systems as shown in Fig. 1a) and b).

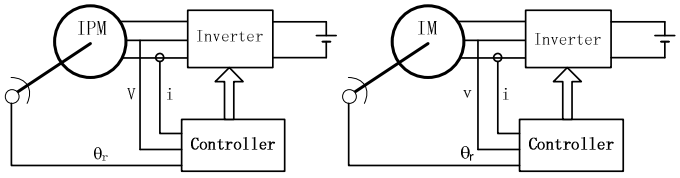

a) IPM Motor and System b) Induction Motor and System

Fig. 1. Popular motors and system in HEV/EV applications

As illustrated in the Fig. 1 a), an IPM uses an inverter to draw/send power from/to the battery pack. The controller takes in the actual current, voltage and rotor position signals as the feedback inputs to generate control signals to the power inverter to generate the needed voltage so that the needed torque and speed are achieved. Because of its compact size and high torque density, adequate speed-torque range, rugged structure and reliability, rare-earth IPM motors are used as the traction motors in about 85-90% HEV/EV applications presently.

For a singly-fed cage IM used for HEV/EV applications as shown in Fig. 1 b), the stator, the power inverter and controller hardware are very similar to those for IPM motor. The rotor is a laminated core equipped with a short-circuited copper cage for efficiency concerns. The control software for an IM is based on vector (field orientation) or direct torque control principles, using the motor actual current, voltage, and rotor position as the feedback signals. The essential difference of a cage IM from IPM is that a cage IM has no external source for magnetic field. In operation an IM has to rely upon its rotor slip relative to the synchronous speed to generate rotor current for torque production. Therefore, the torque density of a cage IM is lower and size larger than that of an IPM motor. It is also to be noted that below synchronous speed, a cage IM can only be in motoring mode and above, generating mode.

An IPM cross-section and driving characteristics in terms of iq and id components are shown in Fig. 2 a) and b). Due to the strong magnetic field given by the buried rare-earth magnets, IPM motors can be designed more compact than any other types of electric motors with a decent torque capability. For a relatively small speed-torque region, an IPM design can be optimized to achieve very high energy efficiency (~96%). Although it is very difficult to do flux-weakening on rare-earth permanent magnets for higher speeds beyond the base speed, people still use an aggressive demagnetization current to achieve high speed operation with a small gain of reluctance torque. The torque capability of an IPM motor is constrained by the allowable current fed to the stator windings without generating excessive loss/heat both in the IPM and power inverter devices. The speed range of IPM is constrained by the available voltages of the inverter/battery.

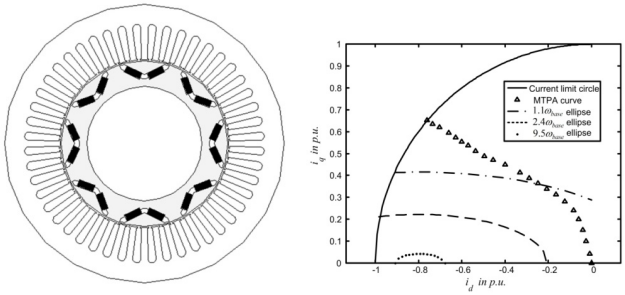

Fig. 2. IPM cross-section and torque characteristics

As shown in Fig. 2 b), the IPM currents are limited by two major factors: a) the thermal limiting circle (solid line) by the thermal stress on IPM windings and inverter devices. If the current magnitude ($\sqrt{i_d{}^2 + i_q{}^2}$) goes beyond this circle, both the IPM and inverter will be overheated; and b) the multiple voltage limiting ellipses (broken lines) by the inverter voltage. The higher of the rotor speed the smaller of the ellipse or less operating area in the i_q-i_d plane. For example, at the speed of 2.4x of the base speed, only the currents within the colored area are achievable though the currents outside the ellipse are still thermally permitted.

Examining the allowed current area, we see that the IPM

current utilization is very different at different speeds. In the low speed region, i_q or torque producing component are dominant and the current well utilized while in high speed region, i_d or demagnetizing component dominant. In the neighborhood of base speed, there exists a Maximum Torque Per Ampere (MTPA) curve or a trajectory for most effective utilization of current (triangle line).

The advantages of an IPM are directly attributed to its use of rare-earth magnets: because of the rare-earth permanent magnets, the magnetic field produced is current-free, and the associated I^2R losses are eliminated, favoring high torque production at speeds below ω_b. The current-free and high strength magnetic field also contributes significantly to the IPM strong torque capability and compact size. For the buried and securely mounted magnets, IPM can also be made for speed above 15,000rpm.

The disadvantages of using rare-earth permanent magnets are obvious: a) rare-earth permanent magnets are very expensive (50X more expensive than cold-rolled steel and 5X copper) and temperature sensitive; b) stiff magnet field produced by rare-earth permanent magnets is very difficult to be weakened for high speed running although needed. In high speed region, 70-80% of the current capacity of the inverter is used for flux weakening purpose, resulting in overheating and low energy efficiency problem (excessive I^2R losses); and c) rare-earth permanent magnets are very geo-politically sensitive.

The cross-section and torque capability of a typical induction motor used in HEV/EV applications are shown in Fig. 3

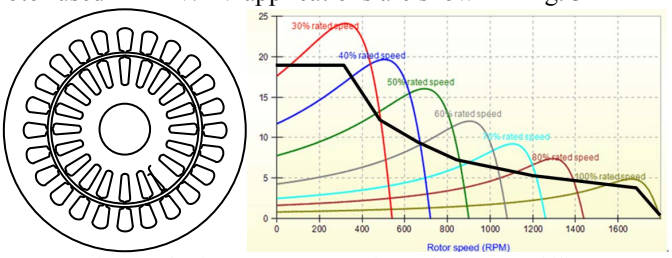

Fig. 3. Induction motor cross-section and torque capability

The mechanical structure of an induction motor is strong and thermally robust as shown in the figure. For energy efficiency improvement, often the cage rotor is made of copper for HEV/EV applications. Compared to an IPM, the torque density of an induction motor is 15-20% less with a slightly larger and heavier motor body. Control of an induction motor is based on the sophisticated field orientation or direct torque control algorithms with decent dynamic torque response. However, speed and torque control of an induction motor is complex and difficult at low speeds (especially zero speed) for its highly nonlinear nature over its speed range.

For overload operation, the peak torque capability of an induction motor is not satisfactory for two reasons: the motor has no external excitation source and the leakage reactance of an induction motor dictates its current for peak torque. Even with a controlled variable drive, at low speed, an induction motor is limited by its pull-out torque that normally is only 1.5 times of the rated value and at high speeds, its torque drops much faster than the rate for constant power operation and when the slip approaching the pull-out frequency, constant power operation is lost. At this point and higher speed, an induction motor is not able to achieve constant power operation. For this reason, an induction motor usually has only a ratio of 1:2 base to maximum speed.

Additionally, a singly fed cage induction motor can only be operated as a motor in sub synchronous speeds and generator super synchronous speed. For this reason, in designing an induction motor, neither can the rated slip frequency be too large (>3%) nor too small (<0.5%). Otherwise the motor energy efficiency suffers or stability becomes a problem.

Doubly-fed motor for HEV/EV application is its much enhanced torque-speed capabilities as that only be found for wound rotor induction machine. For comparison purpose, we assume that there is a normal constant torque region for a comparable IPM or IM defined by the area of ABCD as shown in Fig. 4.

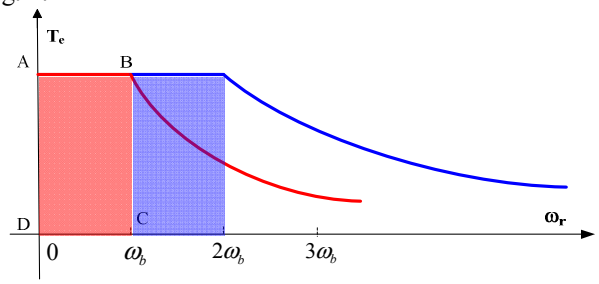

Fig. 4. Comparison of torque-speed region of doubly fed motor to that of singly-fed motor

For higher speeds beyond the base ω_b, IPM or IM has to enter the constant power flux weakening region with higher frequencies. In flux weakening region of IPM, in addition to increasing operating frequency, a large value of negative Id is also required to demagnetize permanent magnets. The applied demagnetization Id reduces the air-gap flux to conform to the maximum inverter voltage but, at the same time, generate excessive copper losses, resulting in lower energy efficiency and overheat problems. The higher speed and larger demagnetizing current the more copper losses and lower efficiency, and at the more reduced torque.

For IM in the higher speed flux weakening operation, the situation is similar except that a reduced magnetizing current Id can be used to weaken air-gap flux. The reduced Id method for flux weakening can be applied without too much trouble for a limited speed range (2 times of ω_b). Further increase of frequency and decrease of Id is not feasible because a dramatically increased rotor slip frequency and rotor copper losses occur. Meanwhile further flux weakening also leads to severely decreased torque production and low energy efficiency.

For a doubly-fed motor, high speed operation is quite different from singly-fed IPMs and IMs. For comparison purpose, we assume that the torque production and base speed of a doubly-fed motor are designed the same as those of the IPM and IM. Going to higher speeds beyond the base ω_b, the doubly-fed motor can maintain the same operational frequency for the first winding while increasing the operating frequency of the other for super synchronous speed operation. The increase of the second winding frequency can go all the way until the induced voltage in the second winding reaching the ceiling of maximum inverter

voltage at $2\omega_b$. The same argument applies to the speed range higher than $2\omega_b$ where the flux weakening and constant power operation starts. In this way, the torque and speed for both constant torque and constant power are all doubled as defined by the blue lines in Fig. 4.

It is worth pointing out that while doubling the torque-speed region, the current levels and, thus, copper losses of both windings are unchanged. Also true is that the stator core losses are not changed while the rotor core losses could be more than that of the IPM and IM but with a big benefit of doubling both the output speed and torque. It is reasonable to derive that a doubly-fed motor will have larger and balanced contour of high energy efficiency than that of both IPM and IM motors, especially at speeds higher than the base speed. A higher energy efficiency of doubly-fed motor in HEV/EV application directly contributes to a better fuel utilization and extended driving distance.

In this paper, a doubly fed motor performance is analyzed and experimentally tested in both steady state and dynamic conditions. The tested results of the doubly fed machine are compared to those for the same motor in the singly-fed conditions. The possibility of eliminating brushes and slip rings for the doubly fed motor is also discussed and solution presented to highlight the bright future of the brushless doubly fed motor in EV/EHV applications.

II. Dynamic Model and Control Strategy for Doubly-Fed Motor

In this section, a control strategy for doubly-fed motor is proposed to address the concern of torque-speed capability, energy efficiency and reliability.

A. System structure and basic equations

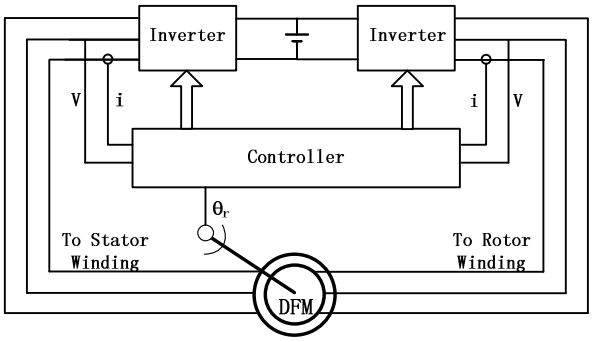

Fig. 5. Doubly-fed motor and system in HEV/EV applications

As shown is Fig. 5, a back to back converter is used for the doubly-fed motor to draw/send power from/to the battery pack. Compared to the power electronic circuits in singly-fed IM and IPM systems, the only difference is the system has two sets of three phases inverter, one connected to stator winding and the other connected to rotor winding. Though the two inverters share the same dc bus, they can be operated separately, meaning that both stator and rotor windings can be controlled independently.

The dynamic equations of doubly fed motor can be written in (1) through (10) as

$$v_{ds} = R_s i_{ds} + \frac{d\lambda_{ds}}{dt} - \omega_s \lambda_{qs} \tag{1}$$

$$v_{qs} = R_s i_{qs} + \frac{d\lambda_{qs}}{dt} + \omega_s \lambda_{ds} \tag{2}$$

$$\lambda_{ds} = L_s i_{ds} + L_m i_{dr} \tag{3}$$

$$\lambda_{qs} = L_s i_{qs} + L_m i_{qr} \tag{4}$$

$$v_{dr} = R_r i_{dr} + \frac{d\lambda_{dr}}{dt} - \omega_r \lambda_{qr} \tag{5}$$

$$v_{qr} = R_r i_{qr} + \frac{d\lambda_{qr}}{dt} + \omega_r \lambda_{dr} \tag{6}$$

$$\lambda_{dr} = L_r i_{dr} + L_m i_{ds} \tag{7}$$

$$\lambda_{qr} = L_r i_{qr} + L_m i_{qs} \tag{8}$$

$$T_e = 1.5p\frac{L_m}{L_s}(\lambda_{qs} i_{dr} - \lambda_{ds} i_{qr}) \tag{9}$$

$$n = \frac{60}{p}(f_s + f_r) \tag{10}$$

The subscripts "s" and "r" refer to the quantities associated with the stator and the rotor windings respectively, v_s and v_r are stator and rotor voltage; i_s and i_r are stator and rotor current; R_s and R_r are stator and rotor resistance; L_m, L_s and L_r are magnetizing, stator and rotor inductance; λ_s and λ_r are stator and rotor flux linkage; ω_s is stator winding electrical angular velocity and ω_r is rotor winding electrical angular velocity; f_s is stator winding electrical frequency and f_r is rotor winding electrical frequency; p is pole pairs and n is rotor mechanical speed. The electromagnetic torque T_e can also be written in another form as

$$T_e = 1.5pL_m(\vec{i}_s \times \vec{i}_r^{\,s'})\sin\delta \tag{11}$$

$$T_e = 1.5pL_m i_s i_r^{s'} \sin\delta \tag{12}$$

where $i_r^{s'}$ is the rotor current referring to stator side, including the magnitude and frequency conversion. The angle δ represents the difference in space between the current vectors $\vec{i}_s$ and $\vec{i}_r^{\,s'}$.

Based on Eqs. (1) through (8), the simplified doubly-fed motor equivalent circuit is shown Fig. 6. In the equivalent circuit I_m is the magnetizing current and the relationship among the currents is represented as a vector equation,

$$\vec{i}_m = \vec{i}_S - \vec{i}_r^{\,s'} \tag{13}$$

Then, the air-gap flux is obtained

$$\lambda_{ag} = L_m i_m \tag{14}$$

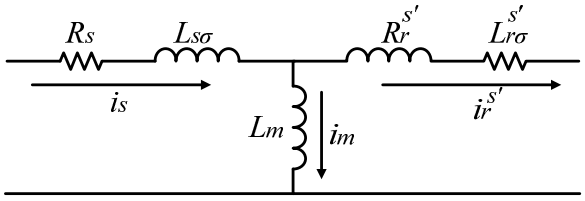

Fig. 6. Doubly-fed motor equivalent circuit

B. *Control algorithm*

According to the characteristics of doubly-fed motor, there are 4-degrees of freedom available for controlling the doubly-fed machine, i_{ds} , i_{qs} , i_{dr} and i_{qr} . Thus, three control objectives can be achieved. Torque is the essence of dynamic performance. In addition, the air-gap flux and Maximum Torque Per Ampere are also the essence for motor efficiency, especially in EV/EHV applications. Based on the torque-speed characteristics described in Fig. 2, the following control algorithm is designed as the principles:

a) The doubly-fed motor is always operated in super synchronous speed, though it can be operated in sub synchronous speed or synchronous speed. The main reason is that the speed range is doubled compared to a singly-fed motor as shown in Fig. 2. In this way, before entering the flux weakening region, a singly-fed motor can only reach while with the same dc bus voltage, the doubly-fed motor can achieve up to $2\omega_b$.

b) Before entering the flux weakening region, to enhance iron core utilization, the control algorithm adjusts the angle δ such that we keep the air-gap flux as the maximum allowable value of the air-gap flux. Whenever entering the flux weakening region, we adjust the angle δ to reduce the air-gap flux to a desired level, consistent with the DC bus voltage. In this way, there is no need to apply a negative i_d that is always required in controlling an IPM.

According to Eqs. (12) through (14), the torque demand can be satisfied by different combinations of i_s , $i_r^{s'}$ and δ ; the proper magnetizing current is produced by vector $\vec{i}_s$ and $\vec{i}_r^{s'}$. Therefore, the torque and air-gap flux in the doubly fed motor can be controlled separately, not just in constant torque but also in flux weakening regions. Once entering the flux weakening region, we can adjust the value of δ to reduce the air gap flux. At the same time satisfactory torque is achieved. The control algorithm can be expressed by the block diagram shown in Fig. 7.

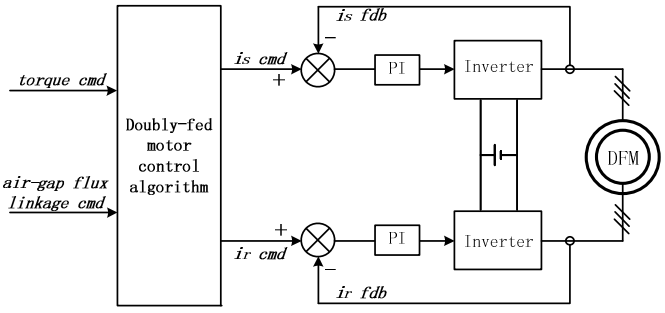

Fig. 7. Block diagram of doubly-fed motor drive system

III. Experimental Testing Verification

In this section, experimental results are presented to verify the algorithm discussed in the above section. The ratings and parameters of doubly-fed motor under testing are listed in TABLE I.

TABLE I
Ratings And Parameters For Prototype Doubly-Fed Motor

Nominal power	1 hp
Nominal stator line-to-line voltage	230 V
Nominal rotor line-to-line voltage	90 V
Nominal stator phase current	3.6 A
Nominal rotor phase current	6.0 A
Number of pole pairs	2
Top speed	1800 rpm
Stator resistance	2.85 Ω
Rotor resistance	1.25 Ω
Stator leakage inductance	22.44 mH
Rotor leakage inductance	12.79 mH
Mutual inductance	164.56 mH

Fig. 8 shows the lab setup of the doubly-fed motor system for experimental testing, including the doubly-fed motor, the back to back converters and DSP based controller.

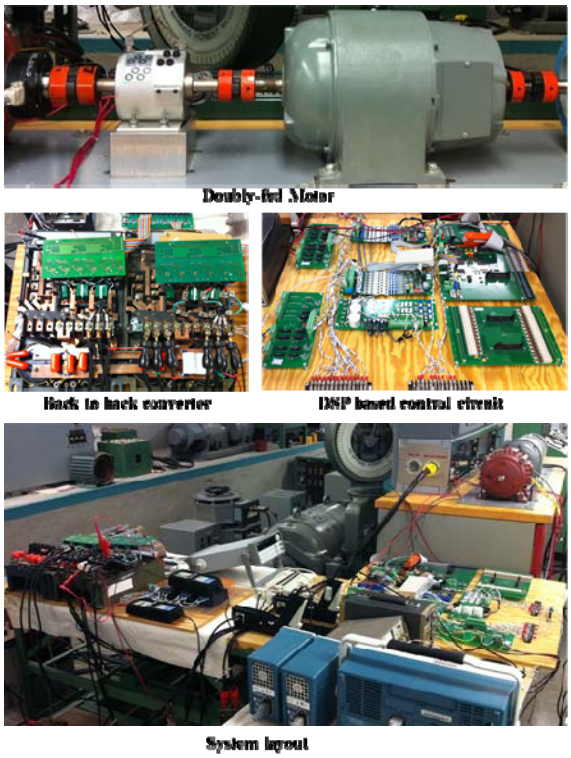

Fig. 8. Doubly-fed motor system

TABLE II summarizes the efficiency comparison results between singly-fed motor and doubly-fed motor, at four typical operating points in steady state condition. The first two tested points are located in the constant torque region, the third one is in the constant power region; the fourth one is not achievable by the machine in the singled-fed mode due to a large dc bus requirement but can be achieved in doubly-fed mode. For this experiment, the tests are conducted on the same motor with two different operational modes, shown in Fig. 1 b) and Fig. 5 respectively. Performance in power efficiency is calculated based on the testing results with converter losses excluded. Based on the results, it is clear that when the motor is operated in the doubly-fed mode, it has a higher efficiency than that for the motor operated in singly-fed mode. In addition, compared to the single-fed mode, the dc bus usage in doubly-fed mode is halved.

TABLE II
COMPARISON OF EFFICIENCY BETWEEN
SINGLY-FED MOTOR AND DOUBLY-FED MOTOR

Speed (rpm)	Torque (N·m)	Singly-fed motor		Doubly-fed motor	
		Efficiency	DC bus (V)	Efficiency	DC bus (V)
900	4.33	63.8%	250	72.4%	125
1200	4.29	74.1%	300	84.1%	150
1700	2.92	59.3%	400	78.4%	200
1700	5.02	Beyond operation region		89.1%	200

The dynamic performance of the doubly-fed motor is shown in Fig. 9. The recorded trace of Channel 1 is the rotor phase current, Channel 2 the stator phase current, Channel 3 the actual speed feedback and Channel 4 the speed reference. As shown in the figure, the doubly-fed motor displays very dynamic speed tracking performance with a speed range from +1800 rpm to -1800 rpm.

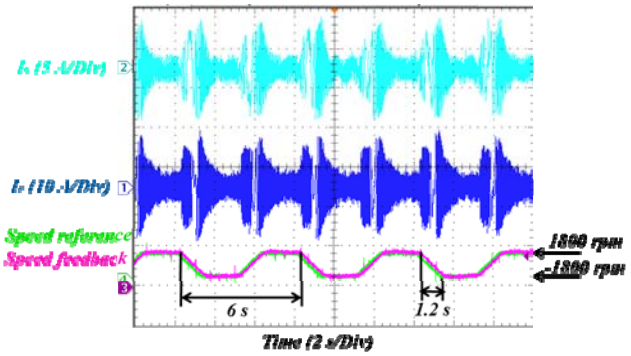

Fig. 9. Experimental waveform of doubly-fed motor variable-speed tracking

IV. CONCLUSIONS

The dynamic model of the doubly-fed is presented and analyzed. With the theoretical background of the doubly-fed machine clarified and compared to those of a singly-fed machine, the control algorithms and strategies suitable for the doubly fed motor are presented. The control algorithms are implemented using a DSP real-time control system and a lab testing bed is set up to carry out an experimental investigation. The experimental testing is conducted on the same motor with singly-fed and doubly-fed modes. Both efficiency in steady state and dynamic response to a speed profile were recorded for comparison studies. The testing results verified that for the same motor, if it is controlled in a singly-fed motor, the energy efficiency of the motor is lower than that in doubly-fed mode. The doubly fed motor can also reach operating point in the torque-speed region where the singly-fed motor not achievable. For dynamic speed tracking, the doubly-fed motor displays very satisfactory results.

It is noticed that for a conventional doubly fed motor, it requires brushes and slip rings to connect the rotor windings to the associated power inverter. However, in our previous research, it has been shown that a brushless doubly fed motor can be designed and controlled in a similar manner as that of the conventional doubly fed induction motor. In this way, it is possible that while eliminating brushes and slip rings, the advantages of a doubly fed motor can be retained. It is quite possible that the brushless doubly fed motor in EV/EHV applications will become a reality.

REFERENCES

[1] L. Xu, "Analysis of a Doubly-Excited Brushless Reluctance Machine by Finite Element Method", IEEE Industry Application Society Annual Meeting, 1992, Houston, Vol.1, pp.171-177.

[2] Y. Liao, L. Xu and L. Zhen, "Design of a doubly fed reluctance motor for adjustable-speed drives", IEEE Transactions on Industry Applications, Vol. 32, No. 5, 1996, pp. 1195-1203.

[3] L. Xu, F. Liang and T. A. Lipo, "Analysis of a New Variable Speed Doubly Excited Reluctance Motor", Electric Machines and Power Systems, Vol. 19. No. 2, March 1991, pp. 125-138.

[4] R. Li, A. Wallace, and Rene Spee, "Dynamic Simulation of Brushless Doubly-Fed Machines", IEEE Transaction on Energy Conversion, Vol. 6, No. 3 September, 1991, pp.445-451.

[5] C.Brune, R. A. K. Wallace, "Experimental Evaluation of A Variable Speed Doubly-Fed Wind-Power Generation System," in Proc.1993 IEEE idustry Applications Society Conf., pp.480-487.

[6] Huijuan Liu and L. Xu, "Comparison study of Doubly Excited Brushless Reluctance Machine with different rotor pole numbers", International Conference on Power Electronics and Motion Control, 2009. IPEMC '09. Wuhan China. 17-20 May 2009, pp.830-835.